THE BELL SYSTEM TECHNICAL JOURNAL
Vol. 60, No. 9 November 1981
Printed in U.S.A.

Adaptive Equalization and Phase Tracking for Simultaneous Analog/Digital Data Transmission

By T. L. LIM and M. S. MUELLER

(Manuscript received May 14, 1981)

The general problem of equalization for data transmission where one of the two data sources produces continuous amplitude data samples is studied. There are various ways to configure a modem for such a transmission scheme, and we describe how a standard quadrature amplitude modulation structure can be modified to operate in this mode. This solution can be specialized to include various linear modulation schemes, such as single sideband and vestigial sideband. Theoretical analysis shows that adaptive equalization and adaptive phase tracking can be achieved with similar quality as in the familiar digital-only modem. We provide extensive computer simulation results which confirm the validity of our theory.

I. INTRODUCTION

Recently, considerable interest arose in finding ways to transmit and receive digital and analog data simultaneously over the 2-wire voiceband telephone channel. We investigate a system using quadrature amplitude modulation (QAM) where digital and analog data modulate the two quadrature channels. The same scheme was independently proposed in Ref. 1. The effects of various channel impairments, as well as an imbalance of signal powers between the digital and analog signals, on the error probability of the system has been studied in Ref. 2.

In this paper, we analyze an adaptive equalizer for this type of hybrid modulation, using a cross-coupled transversal filter as described in detail by Falconer in Refs. 3 and 4. The difference here is that one of the two quadrature channels transmits analog, i.e. continuous amplitude, data. If the communication channel is time invariant, it is possible to train the equalizer with digital data on both quadrature

channels and freeze the equalizer taps after convergence. Analog data can then be sent. However, possible changes in channel characteristics warrant the use of an adaptive equalizer to update the taps continually. Since references for the analog data are not available, especially when the receiver is in a decision-directed mode, the update algorithms reported in Refs. 3, 4 are not applicable in this case. We propose a modification which only minimizes the mean-square error (mse) in the digital data path. Thus, only the error signal from this path is required for adaption. This analysis is similar to that in Refs. 5 and 6.

Results from computer simulations are given to verify our analytical results. We observed that because the analog data does not aid in the equalization, it actually acts as an interferer. As such, it would seem advantageous to reduce the analog signal power, thus, unbalancing the system. On the other hand, this would degrade the analog s/n. Therefore, there is a trade off in allocating different power levels to the two channels depending on which signal is more important.

In the scheme described here, we assume that data symbols are sent every T seconds. Thus, the analog signal has to be limited in bandwidth to $1/(2T)$ in order to avoid aliasing. Alternatively, the two quadrature channels can be used to transmit primarily analog data with occasional digital data for purposes of equalizer updating. Then we could have one high-rate analog channel and a low data rate digital channel.

II. MATHEMATICAL MODEL

The general QAM transmission scheme of Fig. 1 is considered. Two data sequences, $\{a_n\}$ and $\{b_n\}$, are applied to the in-phase and quadrature inputs of the cross-coupled transmission filters with impulse responses $g_p(t)$ and $g_q(t)$. Their output signals are modulated by sine and cosine waves of carrier frequency ω_0 to form the passband signal

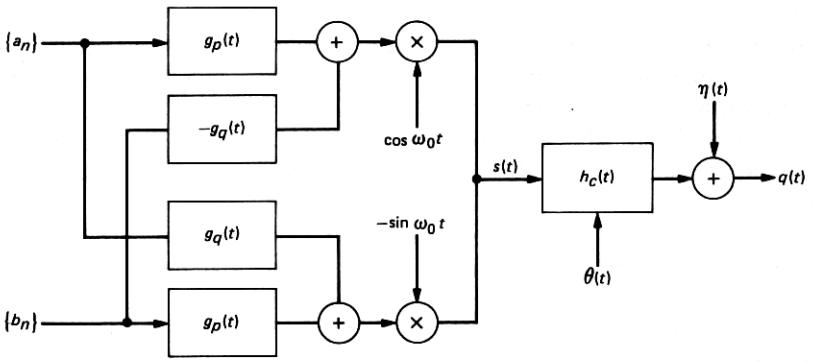

Fig. 1—Model of transmitter and channel.

$$s(t) = \mathrm{Re}\left[\sum_n D_n G(t - nT)\exp(j\omega_0 t)\right], \tag{1}$$

where T is the symbol interval,

$$D_n = a_n + jb_n \tag{2}$$

and

$$G(t) = g_p(t) + jg_q(t). \tag{3}$$

In the above equations, $\{D_n\}$ is the complex sequence of data symbols and $G(t)$ is the complex impulse response of the transmission filter. These parameters can be specialized to represent any linear modulation scheme,[7] e.g., amplitude/phase modulation, single sideband (SSB), vestigial sideband (VSB), and QAM.

Throughout this paper it will be assumed that at least one data sequence, for example, $\{a_n\}$ is digital. In particular, we will report results for a system with $G(t)$ real and where $\{a_n\}$ and $\{b_n\}$ are digital and analog data sequences, respectively. These sequences are assumed to have zero-mean and the following correlation properties:

$$E\{a_n a_m\} = P_a \delta_{nm} \tag{4a}$$

$$E\{b_n b_m\} = P_b \delta_{nm} \tag{4b}$$

$$E\{a_n b_m\} = 0 \tag{4c}$$

$$\delta_{nm} = \begin{cases} 1, & n = m \\ 0, & \text{otherwise} \end{cases}.$$

After passing through a noisy, dispersive, and phase-jittered channel, the signal at the input to the receiver can be expressed as

$$q(t) = \mathrm{Re}\left(\exp\{j[\omega_0 t + \theta(t)]\}\sum_k D_k U(t - kT)\right) + \eta(t),$$

where $U(t)$ is the combined complex impulse response of the transmitting filter and the baseband component of the pass-band channel $h_c(t)$ with respect to the carrier frequency ω_0. The noise process $\eta(t)$ is independent of the data sequences, while the phase shift $\theta(t)$ caused by the channel is assumed to vary much more slowly than the channel-impulse response, $h_c(t)$, and is typically about 10 degrees peak-to-peak. It is mutually independent of the additive noise process, as well as of the data symbols.

The general QAM receiver is shown in Fig. 2. The received signal $q(t)$ is bandpass-filtered by the phase splitter pair with impulse response $F(t) = f(t) + j\check{f}(t)$ where $\check{f}(t)$ denotes the Hilbert transform of $f(t)$.

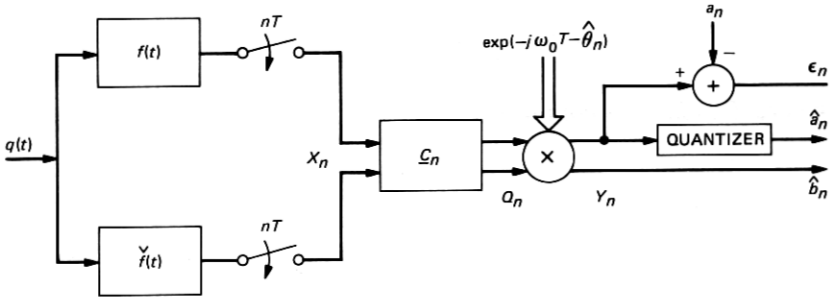

Fig. 2—Receiver structure.

The pair of outputs of the phase splitter at time kT is written as the complex signal sample

$$\begin{aligned} X_k &= x_k + j\check{x}_k \\ &= \exp[j(\omega_0 kT + \theta_k)] \sum_l D_l H_{k-l} + N_k, \end{aligned} \tag{5}$$

where $\{H_k = H(\tau + kT)\}$ are the samples of the overall complex baseband equivalent impulse response, and $\{N_k\}$ are the complex samples of the filtered-noise process. The latter process is uncorrelated with the signal and has an autocorrelation R_{NN}. Thus, we have

$$E\{N_n N_m^*\} = R_{NN}[(n-m)T] \tag{6a}$$

$$E\{N_n N_m\} = 0 \tag{6b}$$

$$E\{a_n N_m\} = 0 \tag{6c}$$

$$E\{b_n N_m\} = 0 \tag{6d}$$

for all integers n and m.

The complex signal sequence $\{X_k\}$ is passed through a cross-coupled passband equalizer with $2M + 1$ complex taps, the output of which at time nT is given by

$$\begin{aligned} Q_n &= \sum_{k=-M}^{M} C_k^* X_{n-k} \\ &= \underline{C}^* \underline{X}_n, \end{aligned} \tag{7}$$

where we write the complex tap as

$$C_k = c_k + j\check{c}_k, \qquad c_k \text{ and } \check{c}_k \text{ real}$$

and define the vectors

$$\underline{C}^t = [C_{-M}, \cdots, C_M] \tag{8}$$

$$\underline{X}_n^t = [X_{n+M}, \cdots, X_{n-M}]. \tag{9}$$

We use the * to denote conjugation for scalars and conjugate transposition for vectors and matrices. The symbol t denotes transposition.

The signal Q_n is demodulated to baseband by multiplication with $\exp(-j\hat{\theta}_n - j\omega_0 nT)$, where $\hat{\theta}_n$ is the estimated phase offset (or jitter) at time nT. The resulting signal Y_n can then be written as

$$Y_n = Q_n \exp(-j\hat{\theta}_n - j\omega_0 nT) \tag{10a}$$

$$= y_n + j\check{y}_n. \tag{10b}$$

The demodulated outputs y_n and $\check{y}_n$ are estimates of the transmitted data samples. In the following section, an optimum equalizer tap vector is derived which minimizes the mse of an appropriate cost function.

III. OPTIMIZATION OF EQUALIZER COEFFICIENTS

3.1 Analysis of the minimum mse criterion for the in-phase branch

In Refs. 3 and 4 an optimum equalizer that minimizes an mse criterion was derived. The mse was defined as

$$E[|Y_n - D_n|^2] = E[\mathrm{Re}^2(Y_n - D_n) + \mathrm{Im}^2(Y_n - D_n)]$$

$$= E[(y_n - a_n)^2] + E[(\check{y}_n - b_n)^2], \tag{11}$$

which is the sum of the mse's in both branches of the equalizer output. It was found that the optimum equalizer coefficients can be calculated adaptively provided the complex output error $Y_n - D_n$ is available to the receiver. While this is the case for a transmission system with digital data in both branches where references can be estimated easily, it is not for the system considered here. In this application only one reference sequence is assumed to be available. Consequently, only the error signal in this branch can be made available for updating purposes.

In the following discussion, we define an optimum tap vector which minimizes the mse in that branch where a reference signal is available or can be estimated easily. The resulting tap vector will be compared with the result for the case where both references are available. Assuming we have a reference for $\{a_n\}$, we define the mse in that branch as the cost function to be minimized

$$\epsilon_n^2 = E[(y_n - a_n)^2] \tag{12}$$

with

$$y_n = \mathrm{Re}[\underline{C}^* \underline{X}_n \exp(-j\hat{\theta}_n - j\omega_0 nT)]. \tag{13}$$

It is convenient to express y_n in vector-matrix notation as follows:

$$y_n = \mathbf{C}^t T(\Delta\theta_n)\mathbf{X}_n, \tag{14}$$

where we partitioned the complex vectors $\underline{C}$ of the passband equalizer

coefficients and $\underline{X}_n \exp(-j\theta_n - j\omega_0 nT)$ of the ideally demodulated received signal to get real vectors $\mathbf{C}$ and $\mathbf{X}_n$ with twice the original dimension

$$\mathbf{C}^t = [\mathrm{Re}(\underline{C}^t) \,|\, \mathrm{Im}(\underline{C}^t)] \tag{15}$$

$$\mathbf{X}_n^t = \{\mathrm{Re}[\underline{X}_n^t \exp(-j\theta_n - j\omega_0 nT)] = |\,\mathrm{Im}[\underline{X}_n^t \exp(-j\theta_n - j\omega_0 nT)]\} \tag{16}$$

$$\Delta\theta_n = \theta_n - \hat{\theta}_n. \tag{17}$$

In eq. (14), $T(\Delta\theta)$ is a transformation matrix expressing the effect of the demodulating phase error $\Delta\theta_n$ and is defined as

$$T(\alpha) = \left[\begin{array}{cc|cc} \cos\alpha & & 0 & -\sin\alpha & & 0 \\ & \ddots & & & \ddots & \\ 0 & & \cos\alpha & 0 & & -\sin\alpha \\ \hline \sin\alpha & & 0 & \cos\alpha & & 0 \\ & \ddots & & & \ddots & \\ 0 & & \sin\alpha & 0 & & \cos\alpha \end{array}\right]. \tag{18}$$

Note that this matrix is orthogonal; that is,

$$T(\alpha) \times T^t(\alpha) = T^t(\alpha) \times T(\alpha) = I. \tag{18a}$$

Furthermore,

$$T(-\alpha) = T^t(\alpha) \tag{18b}$$

and

$$T(\alpha + \beta) = T(\alpha) \times T(\beta) = T(\beta) \times T(\alpha). \tag{18c}$$

In order to get the mse eq. (12) as an explicit function of the coefficient vector $\mathbf{C}$, we introduce the autocorrelation matrix $\mathbf{A}$ of the demodulated received signal

$$\mathbf{A} = E\{\mathbf{X}_n \mathbf{X}_n^t\} \tag{19}$$

and the cross-correlation vector $\mathbf{V}$ between the demodulated received signal and the reference

$$\mathbf{V} = E(\mathbf{X}_n a_n). \tag{20}$$

With eqs. (14), (19), and (20), we can express eq. (12) as follows:

$$\epsilon_n^2 = \mathbf{C}^t T(\Delta\theta_n) \mathbf{A} T(-\Delta\theta_n) \mathbf{C} - 2\mathbf{C}^t T(\Delta\theta_n) \mathbf{V} + E(a_n^2). \tag{21}$$

Setting the partial derivatives with respect to $\mathbf{C}$ to zero yields the vector equation for the optimum tap vector $\mathbf{C}_{\mathrm{opt}}$

$$\mathbf{A} T(-\Delta\theta_n) \mathbf{C}_{\mathrm{opt}} = \mathbf{V}. \tag{22}$$

The definition of $\mathbf{A}$ in eq. (19) ensures that it is positive definite. Consequently, the equation has a unique solution.

$$\mathbf{C}_{\text{opt}} = T(\Delta\theta_n)\mathbf{A}^{-1}\mathbf{V}. \tag{23}$$

Inserting eq. (23) into eq. (21) yields for the minimum mse

$$\epsilon^2_{\text{opt}} = E(a_n^2) - \mathbf{C}^t_{\text{opt}}\, T(\Delta\theta_n)\mathbf{V} = E(a_n^2) - \mathbf{V}\mathbf{A}^{-1}\mathbf{V}. \tag{24}$$

In Appendix A, we show that, for stationary data sequences $\{a_n\}$ and $\{b_n\}$ uncorrelated with the noise, the autocorrelation matrix $\mathbf{A}$ and the cross correlation vector $\mathbf{V}$ are independent of the time instant n. It is important to note that the minimum mse is independent of the constant demodulation phase error $\Delta\theta_n$. This is a consequence of eq. (23) and indicates that even by minimizing the mse in one of the two equalizer outputs, the optimum coefficient vectors can take care of any phase error, in the same manner as in a cross-coupled equalizer which minimizes the total mse at the output.

These facts have been reported in Refs. 5 and 6 for VSB- and SSB-modulated pulse amplitude modulation signals. Our analysis shows, however, that this holds in general for stationary sequences $\{a_n\}$ and $\{b_n\}$. Thus, the independence of the minimum mse on the demodulation phase is a property of the cross-coupled equalizer which is not adversely affected by the particular selection of the cost function nor by the nature of the sequence $\{b_n\}$.

When the power of the two data sequences is balanced, i.e., $P_a = P_b$, it can be seen from eq. (80) that the resulting equation for the optimum tap vector coincides exactly with the equation resulting from minimizing the total mse in both branches. In this case, both methods will give the same optimal coefficient vector and the same total mse.

In all our analysis we have assumed uncorrelated data as described by eqs. (4a) through (4c). If, instead of eq. (4b), we have

$$E(b_n b_m) = R_b(n - m),$$

then the expressions for $\mathbf{A}_1(k, l)$ and $\mathbf{A}_2(k, l)$ in Appendix A would be more complicated but they would remain stationary matrices. Then, assuming correlated data, eq. (24) is in general still valid, except that $\mathbf{V}$ and $\mathbf{A}$ are more complicated than the expressions derived in Appendix A.

Although we have based our analysis on a symbol spaced equalizer, we can also handle fractional spacing and derive similar results. As an example, we can view the $T/2$ equalizer as two parallel symbol-spaced equalizers, where the first of the two data samples during each baud is processed by one of the equalizers while the second is processed by the other equalizer. Let us denote the two equalizer tap vectors as $\underline{C}_1$ and

$\underline{C}_2$ and the input vectors as $\underline{X}_n$ and $\underline{X}_{n+1/2}$. Then we can define

$$\mathbf{C}^t = [\mathrm{Re}(C_1^t)\,|\,\mathrm{Im}(\underline{C}_1^t)\,|\,\mathrm{Re}(\underline{C}_2^2)\,|\,\mathrm{Im}(\underline{C}_2^t)]$$

$$\mathbf{X}_n^t = \{\mathrm{Re}[\underline{X}_n^t \exp(-j\theta_n - j\omega_0 nT)]\,|\,\mathrm{Im}[\underline{X}_n^t \exp(-j\theta_n - j\omega_0 nT)]$$
$$|\,\mathrm{Re}[\underline{X}_{n+1/2}^t \exp(-j\theta_n - j\omega_0 nT)]$$
$$|\,\mathrm{Im}[\underline{X}_{n+1/2}^t \exp(-j\theta_n - j\omega_0 nT)]\}$$

$$T(\alpha) = \left[\begin{array}{c|c} T_1(\alpha) & 0 \\ \hline 0 & T_1(\alpha) \end{array}\right],$$

where $T_1(\alpha)$ is given in eq. (18). With these definitions, all the previous results for $\mathbf{C}_{\mathrm{opt}}$ and $\epsilon_{\mathrm{opt}}^2$ in eqs. (23) and (24) follow.

3.2 Mean square error in the quadrature branch

We now analyzed the mse in the second branch of the equalizer. The output of this branch is

$$\check{y}_n = \mathrm{Im}[\underline{C}^* \underline{X}_n \exp(-j\hat{\theta}_n - j\omega_0 nT)]. \tag{25}$$

Since

$$\mathrm{Im}\{\underline{Z}\} = \mathrm{Re}\left[\underline{Z} \exp\left(-j\frac{\pi}{2}\right)\right], \tag{26}$$

we are able to express $\check{y}_n$ in terms of $\mathbf{C}$ and $\mathbf{X}$ defined in eqs. (15) and (16) using the transformation properties in eq. (18)

$$\check{y}_n = \mathbf{C}^t T\left(\Delta\theta_n - \frac{\pi}{2}\right)\mathbf{X}_n. \tag{27}$$

Therefore, the mse in the second branch can be expressed in vector-matrix notation as follows:

$$\check{\epsilon}_n^2 = E[(\check{y}_n - b_n)^2] \tag{28}$$

$$= \mathbf{C}^t T\left(\Delta\theta_n - \frac{\pi}{2}\right)\mathbf{A}T\left(-\Delta\theta_n + \frac{\pi}{2}\right)\mathbf{C}$$

$$-2\mathbf{C}^t T\left(\Delta\theta - \frac{\pi}{2}\right)E(\mathbf{X}_n b_n) + E(b_n^2). \tag{29}$$

Using eq. (18) and an approach similar to eq. (66) through eq. (70) in Appendix A, we show that

$$T\left(-\frac{\pi}{2}\right)E\{\mathbf{X}_n b_n\} = \mathbf{V}(P_b/P_a). \tag{30}$$

On substituting eq. (30) into eq. (29) we obtain

$$\check{\epsilon}_n^2 = \mathbf{C}^t T\left(\Delta\theta_n - \frac{\pi}{2}\right)\mathbf{A}T\left(-\Delta\theta_n + \frac{\pi}{2}\right)\mathbf{C} - 2\mathbf{C}^t T(\Delta\theta_n)\mathbf{V}\frac{P_b}{P_a} + P_b. \quad (31)$$

For the balanced power case, i.e., $P_a = P_b$, Appendix A shows that

$$T\left(-\frac{\pi}{2}\right)\mathbf{A}T\left(\frac{\pi}{2}\right) = \mathbf{A}, \quad (32)$$

and it follows that

$$\check{\epsilon}^2 = \mathbf{C}^t T(\Delta\theta_n)\mathbf{A}T(-\Delta\theta_n)\mathbf{C} - 2\mathbf{C}^t T(\Delta\theta_n)\mathbf{V} + P_a. \quad (33)$$

This is exactly the same expression as for ϵ^2 in eq. (21). Consequently,

$$\check{\epsilon}^2 = \epsilon^2. \quad (34)$$

Thus, we conclude that the mse's in both branches are equal. In this special case, minimizing the mse in one branch also minimizes the mse in the other branch.

3.3 Analysis of an infinitely long equalizer

While the formal solution eq. (24) for the minimum mse already shows the independence of a constant-phase error, it does not reveal anything about the influence of channel parameters (amplitude, or phase distortion) or of the sampling instant. To obtain further insight into this dependence, we analyze an infinite length equalizer.

We show in Appendix B that the resulting minimum mse for an infinite tap equalizer can be written as

$$\epsilon_{\text{opt}}^2 = \frac{TP_a}{2\pi}\int_{-\pi/T}^{\pi/T} \frac{P_b[Z(\omega) + Z(-\omega)] + 1}{4P_aP_bZ(\omega)Z(-\omega) + (P_a + P_b)[Z(\omega) + Z(-\omega)] + 1}\, d\omega, \quad (35)$$

where

$$Z(\omega) = \left|\frac{H_{\text{eq}}(\omega)}{N_{\text{eq}}(\omega)}\right|^2. \quad (36)$$

In eq. (36) $H_{\text{eq}}(\omega)$ is the Fourier transform of the sampled impulse response $H(\tau + kT)$, where τ indicates the sampling instant. It is related to the transfer function $H(\omega)$ as follows:

$$H_{\text{eq}}(\omega) = \frac{\exp(j\omega\tau)}{T}\sum_{k=-\infty}^{\infty} H\left(\omega + k\frac{2\omega}{T}\right)\exp\left(j2\pi k\frac{\tau}{T}\right), \quad (37)$$

and $|N_{eq}(\omega)|^2$ is the baseband component of the noise power spectrum

$$|N_{eq}(\omega)|^2 = \sum_{k=-\infty}^{\infty} R_{NN}(kT) \exp[-j(\omega + \omega_0)kT]. \tag{38}$$

The formula given in eq. (35) can be evaluated for all the different modulation schemes which can be modeled by a linear transmission system. The only frequency-dependent term appearing in eq. (35) is $Z(\omega)$, the s/n of the sampled received signal. According to eq. (37) this will, in general, depend on the sampling instant, τ, and the phase characteristic of the overall channel transfer function, $H(\omega)$. If the sampling theorem is satisfied, i.e., if $H(\omega) = 0$ for all ω outside the interval $[\omega_1, \omega_1 + 2\pi/T]$, where ω_1 is arbitrary, combining eqs. (37) and (36) shows that the minimum mse is only dependent on the amplitude characteristic of the channel transfer function and of the noise power density spectrum. A QAM transmission system with no excess bandwidth is an example; a system transmitting only one data sequence and using VSB-modulation with less than 100 percent excess bandwidth is another, more realistic example. In case of balanced power in the transmitted data sequences, i.e., $P_a = P_b$ or for $Z(\omega)$ symmetric around ω_1, i.e., $Z(\omega + \omega_1) = Z(-\omega + \omega_1)$, the mse is given by,

$$\epsilon^2_{opt}|_{P_a=P_b} = \frac{TP_a}{2\pi} \int_{-\pi/T}^{\pi/T} \frac{d\omega}{2P_aZ(\omega) + 1}. \tag{39}$$

In eq. (100) of Appendix B we show that the partial derivative of ϵ^2_{opt} with respect to P_b is nonnegative. Therefore, an increase in the analog signal power P_b causes an increase in ϵ^2_{opt}. So the analog signal acts as an interferer to the digital signal.

IV. ANALYSIS OF THE GRADIENT ALGORITHM FOR JOINT EQUALIZATION AND PHASE TRACKING

In an adaptive receiver, the equalizer is assumed to know the reference data for startup and to operate in a decision-directed mode when random data is being sent. In either case, the tap weight vector is being updated continuously. Similarly, the phase offset, or jitter, would be continuously tracked in order to remain in synchronism. As Falconer did, in Refs. 3 and 4, we assume gradient algorithms are used in these updatings as follows (C is now time-varying),

$$\mathbf{C}_{n+1} = \mathbf{C}_n - \frac{\beta}{2} \nabla \mathbf{C} \epsilon_n^2 \tag{40a}$$

$$\hat{\theta}_{n+1} = \hat{\theta}_n - \frac{\alpha}{2} \frac{\partial}{\partial \hat{\theta}_n} \epsilon_n^2, \tag{40b}$$

where $\nabla \mathbf{C}\epsilon_n^2$ denotes the gradient of ϵ_n with respect to $\mathbf{C}$.

It can be shown from eq. (21) that

$$\nabla \mathbf{C}\epsilon_n^2 = 2T(\Delta\theta_n)[\mathbf{A}T^t(\Delta\theta_n)\mathbf{C}_n - \mathbf{V}] \tag{41a}$$

and

$$\frac{\partial}{\partial\hat{\theta}_n}\epsilon_n^2 = 2\mathbf{C}_n^t \frac{\partial T}{\partial\hat{\theta}_n}(\Delta\theta_n)[\mathbf{A}T^t(\Delta\theta_n)\mathbf{C}_n - \mathbf{V}]. \tag{41b}$$

Using the definitions of $\mathbf{A}$ in eq. (19) and $\mathbf{V}$ in eq. (20) and substituting eq. (14) we can recast eqs. (41a) and (41b) into

$$\nabla \mathbf{C}_n\epsilon_n^2 = 2E[T(\Delta\theta_n)\mathbf{X}_n(y_n - a_n)] \tag{42a}$$

$$\frac{\partial\epsilon_n^2}{\partial\hat{\theta}_n} = 2E\left[\mathbf{C}_n^t \frac{\partial T(\Delta\theta_n)}{\partial\hat{\theta}_n}\mathbf{X}_n(y_n - a_n)\right]. \tag{42b}$$

Finally, we use another property of the transformation matrix $T(\alpha)$, namely,

$$\frac{\partial T(\alpha+\beta)}{\partial\alpha} = T\left(\alpha + \beta + \frac{\pi}{2}\right),$$

together with eq. (27) to obtain

$$\frac{\partial\epsilon_n^2}{\partial\hat{\theta}_n} = 2E[\check{y}_n(y_n - a_n)]. \tag{42c}$$

Equations (42a) and (42c) can be used to update the equalizer according to eq. (40). Note that all the signals required to update the equalizer are readily available at the receiver. Also note that $y_n - a_n = e_n$ is the error in the branch where a reference is available and $\check{y}_n$ is the output of the other branch.

By taking expected values as shown in eqs. (42a and b), we obtain the estimated gradient algorithm. In practice, a stochastic gradient approach is used to avoid the long delay involved in estimating the averages. The update equations are obtained by omitting the expectations in eq. (42) and making small corrections in the direction of the instantaneous values instead. Hereafter, we shall discuss only the stochastic gradient method.

Inserting eq. (42a) into eq. (40a) yields the update equation for the coefficient vector

$$\mathbf{C}_{n+1} = \mathbf{C}_n - \beta'(y_n - a_n)T(\Delta\theta_n)\mathbf{X}_n. \tag{43}$$

The corresponding equation for the update of the phase jitter corrector is

$$\check{\theta}_{n+1} = \check{\theta}_n - \frac{\alpha'}{a_n^2}\check{y}_n(y_n - a_n). \tag{44}$$

Division by a_n^2 has been included in eq. (44) to give the corrections a smaller weight, if the nominal data value has a larger absolute value. Note that because of the special nature of $T(\Delta\theta_n)$ defined in eq. (18), the matrix multiplication in eq. (43) requires only $2(2M + 1)$ multiplication. Equation (43) can be reexpressed in terms of the complex equalizer $\underline{C}_n$ and input $\underline{X}_n$ as

$$\underline{C}_{n+1} = \underline{C}_n - \beta' \underline{X}_n [(y_n - a_n) \exp(jn\omega_0 T + j\theta_n)]^*. \tag{45}$$

The equalizer coefficient and phase adjustment algorithms represented by eqs. (44) and (45) are similar to the ones published in Ref. 3. The main difference is that here, only the error in the digital data path appears in the adjustment algorithms.

An important parameter in the evaluation of the dynamic behavior of the control loop is the rate of convergence (ROC). For the case of updating the equalizer only, the ROC can be analyzed using, for example, Ungerboeck's method,[8] since the stochastic recurrence equations for the excess mse can be cast in the form analyzed in Ref. 8. Combining eq. (43) with eq. (14), it is seen that for the stochastic gradient case

$$T(-\Delta\theta_n)\mathbf{C}_{n+1} = [I - \beta' \mathbf{X}_n \mathbf{X}_n^t] T(-\Delta\theta_n)\mathbf{C}_n + \beta' a_n \mathbf{X}_n. \tag{46}$$

From eqs. (21) and (24) the excess mse is given by

$$\epsilon_n^2 - \epsilon_{\text{opt}}^2 = (\mathbf{C}_n - \mathbf{C}_{\text{opt}})^t T(\Delta\theta_n) \mathbf{A} T(-\Delta\theta_n)(\mathbf{C}_n - \mathbf{C}_{\text{opt}}). \tag{47}$$

Therefore,

$$\epsilon_{n+1}^2 - \epsilon_{\text{opt}}^2 = \mathbf{D}_n^t \mathbf{A} \mathbf{D}_n, \tag{48}$$

with

$$\mathbf{D}_n = (I - \beta' \mathbf{X}_n \mathbf{X}_n^t) T(-\Delta\theta_n)(\mathbf{C}_n - \mathbf{C}_{\text{opt}}) - \beta' \mathbf{X}_n [\mathbf{X}_n^t T(-\Delta\theta_n)\mathbf{C}_{\text{opt}} - a_n]. \tag{49}$$

The convergence of the excess mse eq. (48) is analyzed in Ref. 8. There it is shown further that for stability the control loop constant has to satisfy

$$0 \le \beta' \le \frac{2}{E(\mathbf{X}_n^t \mathbf{X}_n)}, \tag{50}$$

with

$$\beta_0' = \frac{1}{E(\mathbf{X}_n^t \mathbf{X}_n)}. \tag{51}$$

The control loop constant, β_0', is chosen to give the fastest initial convergence.

In steady-state the excess mse is given by

$$\epsilon_\infty^2 - \epsilon_{\text{opt}}^2 = \frac{\beta' E(\mathbf{X}^t\mathbf{X})\epsilon_{\text{opt}}^2}{2 - B'E(\mathbf{X}^t\mathbf{X})}. \tag{52}$$

From eq. (52) it can be seen that the excess mse can be reduced to an arbitrarily small value by selecting β' small enough.

It is interesting to note that eq. (50) specifies a stability region for β' equal to that for an equalizer using error signals from both branches $[E(\mathbf{X}^t\mathbf{X}) = E(\underline{X}^*\underline{X})]$. From eq. (52) it follows that for a particular β' the ratio of the excess mse to ϵ_{opt}^2 is the same as for an equalizer using error signals from both branches.

We have not been able to analyze the ROC for the joint operation of equalizer and phase jitter loops. In contrast to the equalizer update equation, the transformation matrix $T(\Delta\theta_n)$ in the joint case is involved in a nonlinear manner. We, therefore, resort to computer simulation of the loop behavior. These results are reported in the next section.

V. SIMULATION RESULTS

Here, we present simulation results for the hybrid modulation scheme described earlier. Pseudorandom digital data selected from the $\{\pm 1, \pm 3\}$ alphabet is used to modulate the in-phase channel, while a set of pseudorandom numbers with a Gaussian distribution $N(O, P_b)$ modulates the quadrature channel, where P_b is the analog signal power. Additive Gaussian noise at -30 dB below the average signal level is introduced in the channel and, whenever desired, phase jitter is introduced. The latter process is modeled by a 60-Hz sinusoid of 10 degrees peak-to-peak. The channels used in the simulation are (*i*) a good channel with a flat amplitude frequency response within most of the frequency band of interest and small delay distortion, except near the lower band edge, and (*ii*) a channel just violating the requirements for basic conditioning with both moderate amplitude and delay distortion. These characteristics are shown in Fig. 3.

Although it is not intended to start up an equalizer with a reference signal only in one branch, we report results of such simulations. This gives good insight into the dynamic behavior of the adaptive equalizer update loop and facilitates the comparison with a conventional passband equalizer.

The first run described is for balanced power ($P_a = P_b = 5$), where the receiver has a 64-tap $T/2$ complex equalizer and the error signal is derived from the in-phase digital channel alone. The basic channel described above is used. Figure 4 is a sample simulation run displaying the s/n as a function of time where s/n is defined as the ratio of the digital signal power to the digital mse. The latter is taken to be a weighted sum of past and present instantaneous squared errors. The

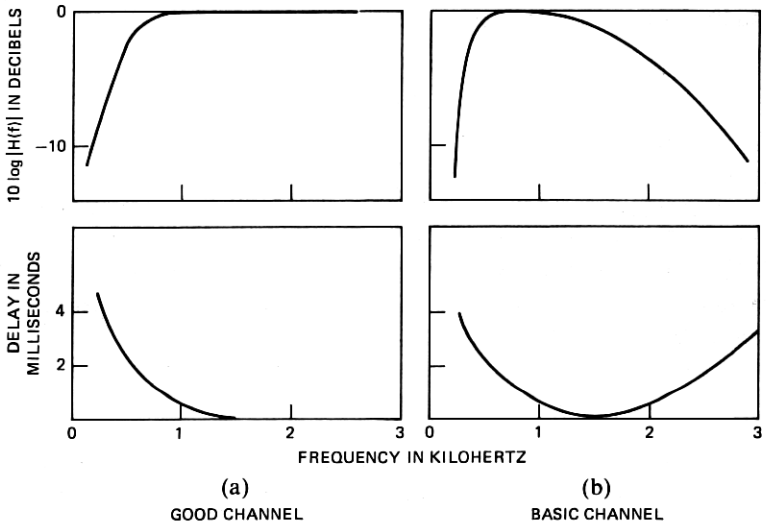

Fig. 3—Channel frequency responses.

two curves are for two different timing phases in the receiver. As shown, the equalizer converges in about 2000 iterations for a step size of $\beta = 0.0005$. The step size giving the fastest convergence, according to eq. (53), would be $\beta_0 = 0.0015$. A lower value is used in order to re-

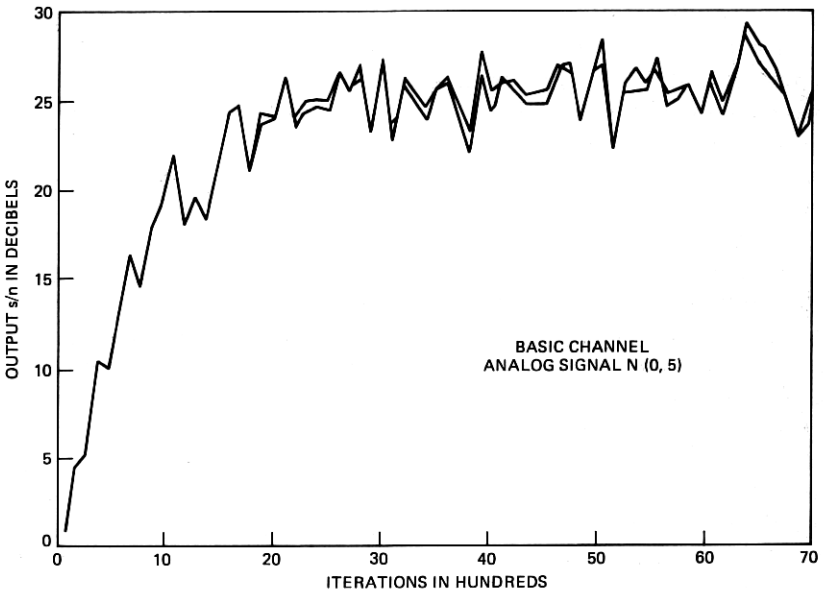

Fig. 4—Convergence of hybrid equalizer.

duce the mse in steady state. The receiver's digital and analog outputs after equalization and demodulation to baseband are displayed in Fig. 5 as a scatter plot. The vertical and horizontal axes represent analog and digital values respectively and, ideally, the data points would be on vertical lines passing through the X-axis at ± 1, ± 3. Owing to channel noise, there is both lateral and vertical displacement from the true values. The decision thresholds for the digital data are the vertical lines with abscissae 0 and ± 2. In this example, and all the others to be described, the input s/n is about 30 dB so that the equalizer has done a reasonable job in removing intersymbol interference (ISI) caused by the basic channel.

We next exhibit the results for the regular QAM in Figs. 6 and 7, with digital data on both branches and using exactly the same channel and receiver parameters as before. The ideal constellation in the scatter plot would be 16 points with coordinates ± 1, ± 3 (in the absence of ISI

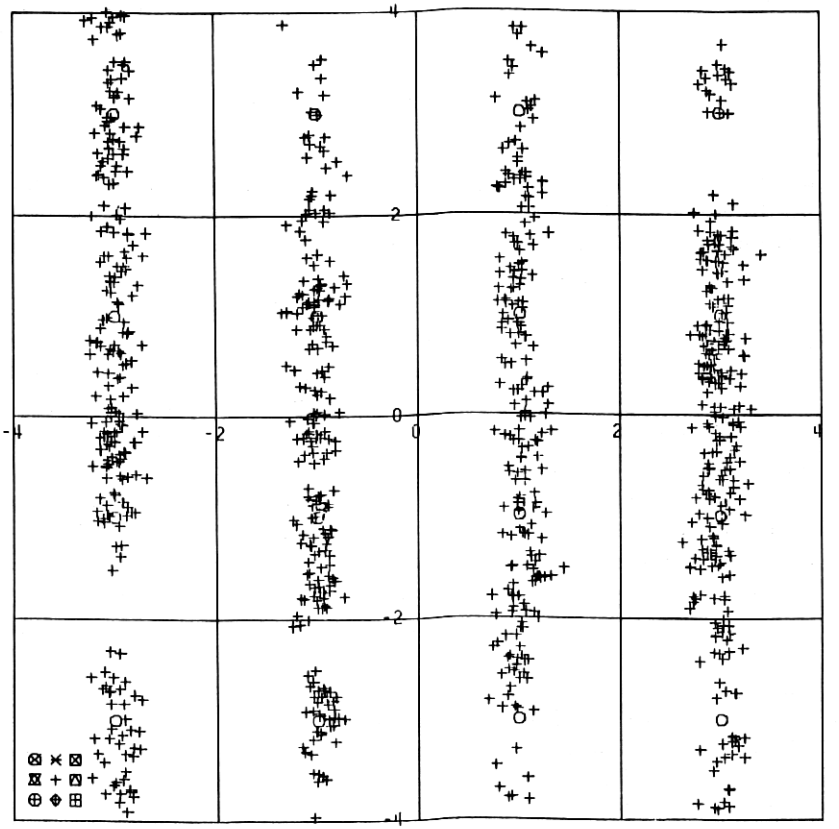

Fig. 5—Hybrid receiver output constellation.

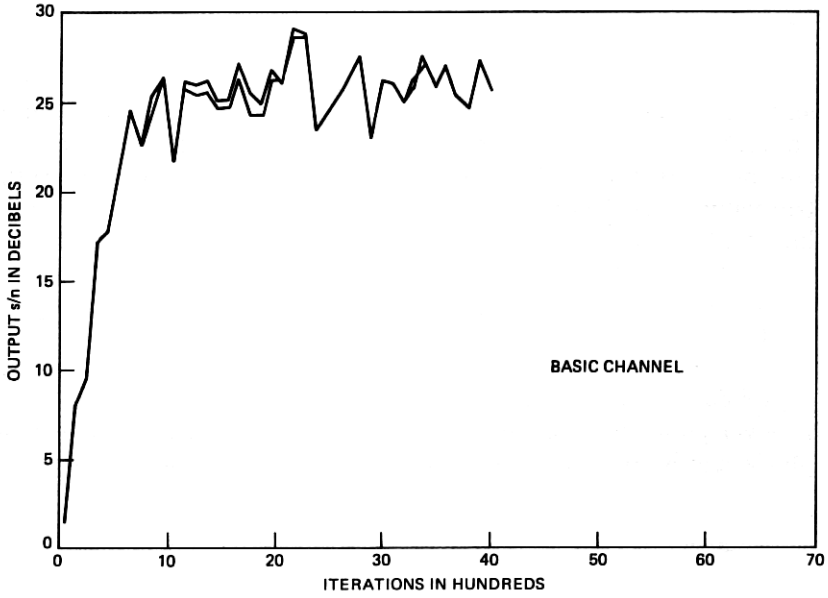

Fig. 6—Convergence of regular QAM equalizer.

and channel noise). As seen in Fig. 6, the convergence is faster than for the hybrid modulation since here we used a complex error function, leading to a tap weight vector $\underline{C}_n$ that fluctuates less than when using a one-sided error signal only.

We mentioned in Section 3.1 that when the powers in the digital and analog branches are balanced, the optimum equalizer and mse are the same as that of a regular QAM receiver. Indeed, we see by comparing Figs. 4 and 6 that the digital mse's reach the same levels. It was also observed that the significant tap weights for both receiver timing phases differ by less than 5 percent.

Now we exhibit the effect on the mse of unbalancing the analog signal power from $P_b = 5$ to some other value. The simulated receiver has an AGC that scales the received signal to an average power of "ten" and, hence, the equalizer tap adjustment step size is kept the same in this series of runs. The analog mse is obtained by averaging all the past instantaneous mse's over time. Instead of presenting a series of curves, we summarize the results in Table I. The digital signal power is fixed at "five," but the analog power is varied from "one" to "nine." The output mse normalized to the power of the corresponding signal is presented in Table I for the good channel. Thus, we see that, as the analog power is increased, the digital mse increases, confirming the analytical results in Section 3.3 for the infinite length equalizer. It was

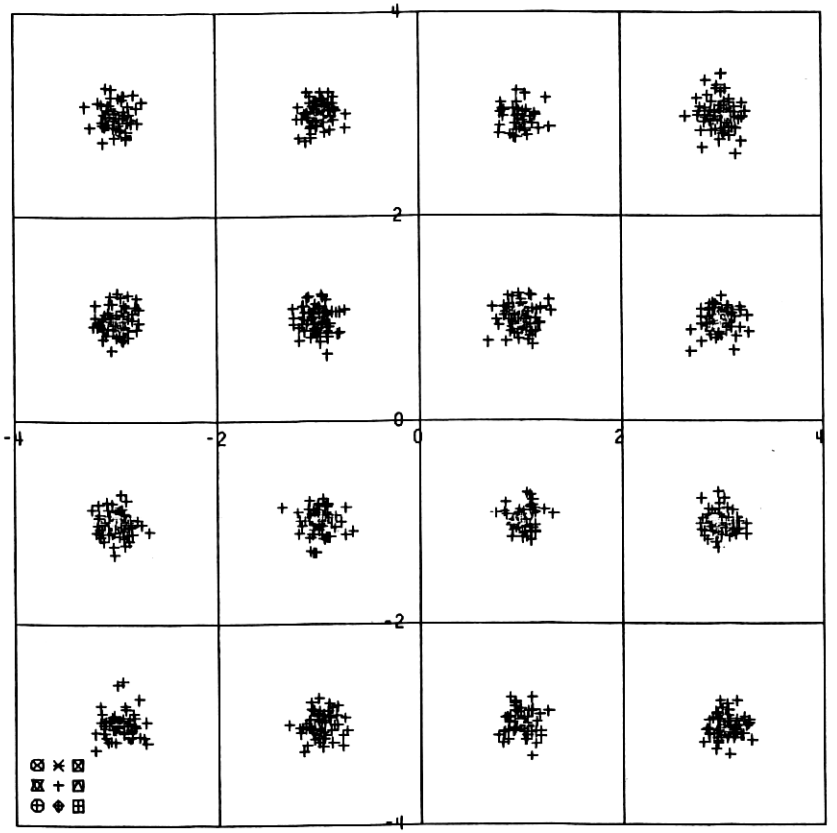

Fig. 7—Regular QAM receiver output constellation.

also shown in Ref. 2 that the error probability upper bound is increased when a power imbalance exists in favor of the analog signal. As expected, we also see that the normalized analog mse is smaller with a larger analog signal power. We also note that the digital and analog

Table I—Comparison of analog and digital mse for different P_b (good channel)

Analog Power P_b	Normalized mse	
	Digital	Analog
1	0.0007	0.0040
3	0.0010	0.0017
5	0.0013	0.0013
7	0.0016	0.0011
9	0.0018	0.0009

mse's are almost the same for balanced power, as theoretically predicted in Section 3.2.

Simulations were also performed to study the hybrid equalizer performance in the presence of sinusoidal phase jitter of 60 Hz, where the phase tracker modeled by eq. (44) is used to estimate the jitter process. Figure 8 shows a sample run where, after allowing the equalizer to reach steady-state, 60-Hz jitter with 10 degrees peak-to-peak amplitude is introduced causing a degradation in performance. The plot in Fig. 9 shows the same run, except that the phase tracker is turned on shortly after the phase jitter is introduced. The lower the jitter frequency and amplitude, the more effective we can expect the phase tracker to be.[4]

VI. CONCLUSION

A data transmission system capable of transmitting and receiving analog and digital data simultaneously has been studied in detail. We found that it is possible to perform adaptive equalization of the channel even when only one of the two quadrature channels is carrying digital data. Moreover, the minimum mse and tap-weight vector are unchanged from that of the regular QAM as long as the analog and digital

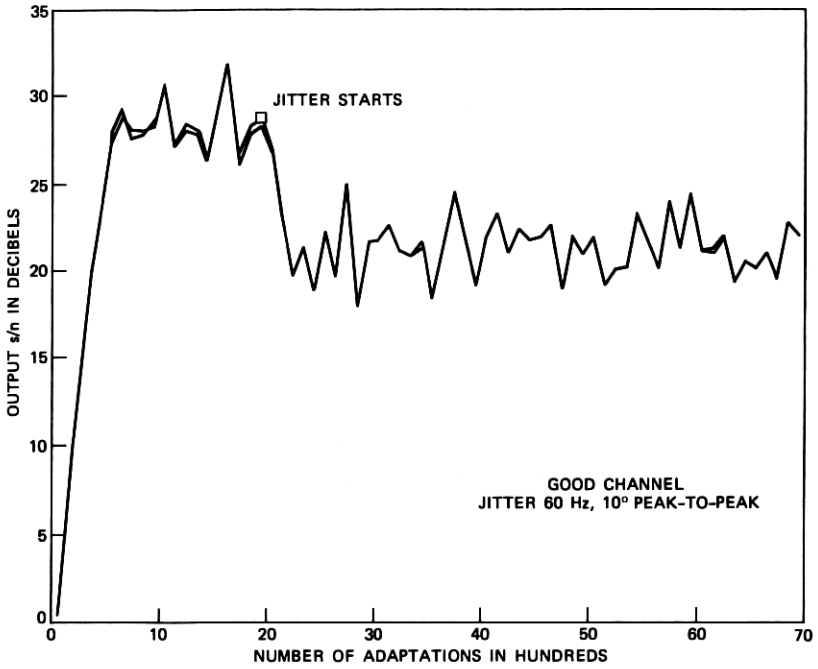

Fig. 8—Hybrid receiver performance in presence of phase jitter (no carrier recovery).

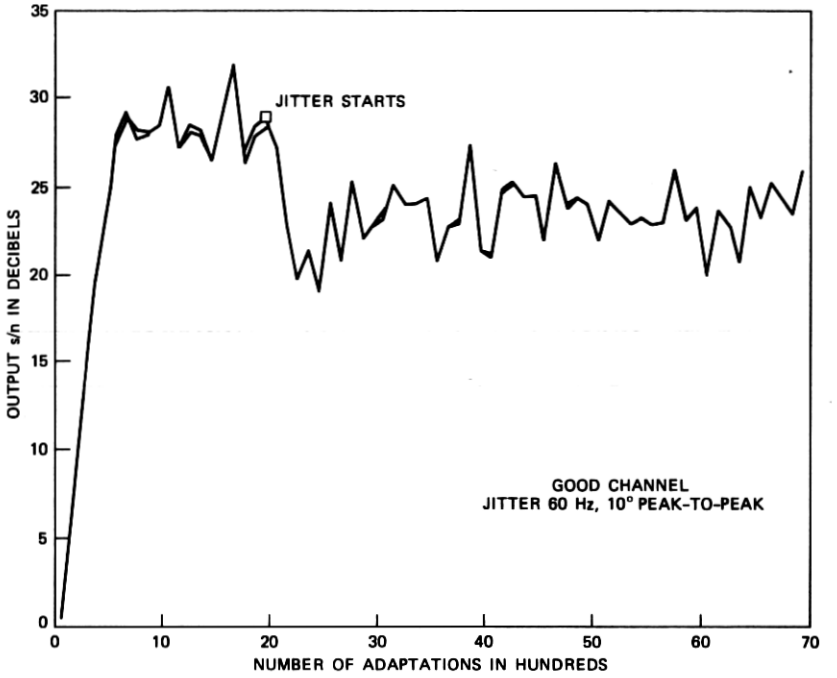

Fig. 9—Hybrid receiver performance in presence of phase jitter (carrier recovery, $\alpha = 0.5$).

signal powers are equal. However, start-up with simultaneous analog and digital data is slower by approximately a factor of two compared to the case of a conventional QAM system. An efficient start-up procedure might be to train the receiver with digital data on both channels and then switch one channel to analog data upon convergence of the equalizer, since in the case of balanced power, the equalizer taps are the same. We also found that the scheme can tolerate moderate amounts of phase jitter.

APPENDIX A

Analysis of A *and* V

We define,

$$\underline{X}_{p,n} = \mathrm{Re}[\underline{X}_n \exp(-j\theta_n - j\omega nT)] \tag{53a}$$

$$\underline{X}_{q,n} = \mathrm{Im}[\underline{X}_n \exp(-j\theta_n - j\omega_0 nT)]. \tag{53b}$$

According to eq. (16), it follows that

$$\mathbf{X}_n^t = (\underline{X}_{p,n}^t | \underline{X}_{q,n}^t). \tag{54}$$

Inserting eq. (54) into the definition eq. (19) of $\mathbf{A}$ yields

$$\mathbf{A} = E\left(\begin{array}{c|c} \underline{X}_{p,n}\underline{X}^t_{p,n} & \underline{X}_{p,n}X^t_{q,n} \\ \hline \underline{X}_{q,n}X^t_{p,n} & \underline{X}_{q,n}X^t_{q,n} \end{array}\right). \tag{55}$$

This can be expressed as

$$\mathbf{A} = \frac{1}{2}\left(\begin{array}{c|c} \mathrm{Re}(\mathbf{A}_1 + \mathbf{A}_2) & -\mathrm{Im}(\mathbf{A}_1 - \mathbf{A}_2) \\ \hline \mathrm{Im}(\mathbf{A}_1 + \mathbf{A}_2) & \mathrm{Re}(\mathbf{A}_1 - \mathbf{A}_2) \end{array}\right), \tag{56}$$

where

$$\mathbf{A}_1 = E[(\underline{X}_{p,n} + j\underline{X}_{q,n})(\underline{X}_{p,n} - j\underline{X}_{q,n})^t] = E(\underline{X}_n\underline{X}^*_n) \tag{57}$$

$$\begin{aligned}\mathbf{A}_2 &= E[(\underline{X}_{p,n} + j\underline{X}_{q,n})(\underline{X}_{p,n} + j\underline{X}_{q,n})^t] \\ &= E[\underline{X}_n\underline{X}^t_n \exp(-2j\theta - 2j\omega_0 nT)].\end{aligned} \tag{58}$$

We note that $\mathbf{A}_2$ is symmetric and $\mathbf{A}_1$ is Hermitian. For uncorrelated data and noise sequences the k, lth entry in the matrix $\mathbf{A}_2$ is computed with eqs. (5), (6), (9), and (58) as follows

$$\begin{aligned}\mathbf{A}_2(k, l) &= E[X_{n-k}X_{n-l}\exp(-2j\theta_n - 2j\omega_0 nT)] \\ &= \sum_\nu \sum_\mu E(D_\nu D_\mu)H_{n-k-\nu}H_{n-l-\mu} \\ &\quad \exp[j(\theta_{n-k} + \theta_{n-l} - 2\theta_n) - j\omega_0(k + l)T] \\ &\quad + E[N_{\mu-k}N_{n-l}\exp(-2j\theta_n - 2j\omega_0 nT)].\end{aligned} \tag{59}$$

From eqs. (2) and (4) we get

$$E(D_\nu D_\mu) = (P_a - P_b)\delta_{\nu\mu}. \tag{60}$$

With the assumption that the phase jitter is quasi-stationary over the equalizer length, i.e. $\theta_{n-k} = \theta_n$ for all $k \in [-M, M]$, we obtain

$$\mathbf{A}_2(k, l) = (P_a - P_b)\sum_\nu H_\nu H_{\nu+k-l}\exp[-j\omega_0(k + l)T]. \tag{61}$$

Note that $\mathbf{A}_2(k, l)$ is zero, if the powers of the sequences $\{a_n\}$ and $\{b_n\}$ are equal, i.e., $P_a = P_b$.

Similarly the k, lth entry in $\mathbf{A}_1$ is

$$\begin{aligned}\mathbf{A}_1(k, l) &= E(X_{n-k}X^*_{n-l}) \\ &= \sum_\nu \sum_\mu E(D_\nu D^*_\mu)H_{n-k-\nu}H^*_{n-l-\mu} \\ &\quad \times \exp[j(\theta_{n-k} - \theta_{n-l}) + j\omega_0(l - k)T] \\ &\quad + E[N_{n-k}N^*_{n-l}],\end{aligned} \tag{62}$$

with

$$E(D_\nu D^*_\mu) = (P_a + P_b)\delta_{\nu\mu}, \tag{63}$$

$$E(N_\nu N_\mu^*) = R_{NN}[(\mu - \nu)T], \tag{64}$$

and the assumption of quasi-stationary phase jitter, this finally yields

$$\mathbf{A}_1(k, l) = (P_a + P_b) \sum_\nu H_\nu H_{\nu+k-l}^* \times \exp[j\omega_0(l-k)T] + R_{NN}[(k-l)T]. \tag{65}$$

With the definition of $\mathbf{V}$ in eqs. (20) and (54), we find

$$\mathbf{V} = E\begin{pmatrix} \underline{X}_{p,n} a_n \\ \underline{X}_{q,n} a_n \end{pmatrix} \tag{66}$$

or

$$\mathbf{V} = \begin{pmatrix} \underline{V}_1 \\ \underline{V}_2 \end{pmatrix}, \tag{67}$$

with

$$\underline{V}_1 = E[\underline{V}_{p,n} a_n] \tag{68a}$$

and

$$\underline{V}_2 = E[\underline{X}_{q,n} a_n]. \tag{68b}$$

The kth entry in $\underline{V}_1$ is calculated by inserting eqs. (5), (9), and (53a) into (68b)

$$\begin{aligned} V_1(k) &= E\{a_n \mathrm{Re}[X_{n-k} \exp(-j\theta_n - j\omega_0 nT)]\} \\ &= E\{a_n \mathrm{Re}[\exp(j\theta_{n-k} - j\theta_n - j\omega_0 kT) \sum_l D_l H_{n-k-l}]\}. \end{aligned} \tag{69}$$

Again, under the assumption of quasi-stationary phase jitter and with eqs. (2) and (4), we have

$$V_1(k) = P_a \mathrm{Re}[H_{-k} \exp(-j\omega_0 kT)]. \tag{70}$$

Following the same lines, one obtains for $V_2(k)$,

$$V_2(k) = P_a \mathrm{Im}[H_{-k} \exp(-j\omega_0 kT)]. \tag{71}$$

A transformed version of $\mathbf{A}$ is needed for the analysis of the mse in the second branch. According to eq. (18), the transformation matrix is

$$T\left(-\frac{\pi}{2}\right) = \left[\begin{array}{ccc|ccc} 0 & & 0 & 1 & & 0 \\ & \ddots & & & \ddots & \\ 0 & & 0 & 0 & & 1 \\ \hline -1 & & 0 & 0 & & 0 \\ & \ddots & & & \ddots & \\ 0 & & -1 & 0 & & 0 \end{array}\right]. \tag{72}$$

Inserting this into eq. (56) yields

$$T\left(-\frac{\pi}{2}\right)\mathbf{A}T\left(\frac{\pi}{2}\right)=\frac{1}{2}\left[\begin{array}{c|c}\mathrm{Re}(\mathbf{A}_1-\mathbf{A}_2) & -\mathrm{Im}(\mathbf{A}_1+\mathbf{A}_2)\\ \hline \mathrm{Im}(\mathbf{A}_1-\mathbf{A}_2) & \mathrm{Re}(\mathbf{A}_1+\mathbf{A}_2)\end{array}\right]. \tag{73}$$

By comparing eq. (73) with eq. (56), it is found that

$$T\left(-\frac{\pi}{2}\right)\mathbf{A}T\left(\frac{\pi}{2}\right)=\mathbf{A}+\mathbf{A}' \tag{74}$$

with

$$\mathbf{A}'=\left[\begin{array}{c|c}-\mathrm{Re}\mathbf{A}_2 & -\mathrm{Im}\mathbf{A}_2\\ \hline -\mathrm{Im}\mathbf{A}_2 & \mathrm{Re}\mathbf{A}_2\end{array}\right]. \tag{75}$$

In eq. 75, $\mathbf{A}'$ is symmetric but not positive definite. Then, referring to eq. (61), we see that for the balanced power case, i.e., $P_a = P_b$,

$$\mathbf{A}'=0 \quad \text{and} \quad T\left(-\frac{\pi}{2}\right)\mathbf{A}T\left(\frac{\pi}{2}\right)=\mathbf{A}.$$

APPENDIX B

Optimum Tap Weight and mse of the Infinitely Long Equalizer

Define

$$\mathbf{C}_{\mathrm{opt}}^{t}=(\underline{C}_1^{t}\mid \underline{C}_2^{t}) \tag{76}$$

and use eqs. (56) and (67). Then, the equation for the optimum coefficient vector eq. (22) can be expressed as follows

$$\begin{aligned}\mathrm{Re}(\mathbf{A}_1+\mathbf{A}_2)\underline{C}_1-\mathrm{Im}(\mathbf{A}_1-\mathbf{A}_2)\underline{C}_2&=2\underline{V}_1\\ \mathrm{Im}(\mathbf{A}_1+\mathbf{A}_2)\underline{C}_1+\mathrm{Re}(\mathbf{A}_1-\mathbf{A}_2)\underline{C}_2&=2\underline{V}_2,\end{aligned} \tag{77}$$

where it is assumed that the demodulation phase error $\Delta\theta_n$ equals zero. (It has been stated that the minimum mmse is independent of $\Delta\theta_n$, at least for a constant phase offset. Therefore, no loss of generality results because of this simplification).

Let

$$\underline{C}=(\underline{C}_1+j\underline{C}_2) \tag{78}$$

and

$$\underline{V}=(\underline{V}_1+j\underline{V}_2). \tag{79}$$

This allows us to write eq. (77) in complex notation

$$\mathbf{A}_1\underline{C}+\mathbf{A}_2\underline{C}^{*}=2\underline{V}. \tag{80}$$

Equation (80) can be expressed in the components of the vector $\underline{V}$ and

matrices $\mathbf{A}_1$ and $\mathbf{A}_2$

$$\sum_{l=-M}^{M} [\mathbf{A}_1(k, l)C(l) + \mathbf{A}_2(k, l)C^*(l)] = 2V(k). \tag{81}$$

Note from eq. (61) that since $\mathbf{A}_2$ is not a Toeplitz matrix, the sum in eq. (81) is not a convolution even if the dimension M approaches infinity. Define

$$\tilde{C}(l) = C(l)\exp(j\omega_0 lT), \tag{82}$$

$$\tilde{V}(l) = V(l)\exp(j\omega_0 lT), \tag{83}$$

$$\begin{aligned}\tilde{\mathbf{A}}_1(k-l) &= \mathbf{A}_1(k, l)\exp[-j\omega_0(l-k)T], \\ &= (P_a + P_b)\sum_{\nu} H_\nu H^*_{\nu+k-l} \\ &\quad + R_{NN}(k-l)\exp[-j\omega_0(l-k)T],\end{aligned} \tag{84}$$

$$\begin{aligned}\tilde{\mathbf{A}}_2(k-l) &= \mathbf{A}_2(k, l)\exp[j\omega_0(k-l)T], \\ &= (P_a - P_b)\sum H_\nu H_{\nu+k-l}.\end{aligned} \tag{85}$$

Equations (61) and (65) were used to get eqs. (84) and (85). With these definitions, we can transform the problem to baseband. Inserting eqs. (82) to (85) into eq. (81) yields

$$\sum_{l=-M}^{M} [\tilde{\mathbf{A}}_1(k-l)\tilde{C}(l) + \tilde{\mathbf{A}}_2(k-l)\tilde{C}^*(l)] = 2\tilde{V}(k). \tag{86}$$

Here the sums will be convolutions if $M \to \infty$. Consequently, the equation can be expressed in the domain of Fourier transform as

$$\tilde{\mathbf{A}}_1(\omega)\tilde{C}(\omega) + \tilde{\mathbf{A}}_2(\omega)\tilde{C}^*(-\omega) = 2\tilde{V}(\omega). \tag{87a}$$

Together with the transform of the conjugate complex of eq. (86), which is

$$\tilde{\mathbf{A}}_1^*(-\omega)C^*(-\omega) + \tilde{\mathbf{A}}_2^*(-\omega)\tilde{C}(\omega) = 2\tilde{V}^*(-\omega), \tag{87b}$$

it can be used to find the formal solution

$$\tilde{C}(\omega) = \frac{2\tilde{V}(\omega)\tilde{\mathbf{A}}_1^*(-\omega) - 2\tilde{V}^*(-\omega)\tilde{\mathbf{A}}_2(\omega)}{\tilde{\mathbf{A}}_1(\omega)\tilde{\mathbf{A}}_1^*(-\omega) - \tilde{\mathbf{A}}_2(\omega)\tilde{\mathbf{A}}_2^*(-\omega)}. \tag{88}$$

The Fourier transform of the sampled impulse response $H(\tau + kT)$, where τ indicates the sampling instant, is defined as follows

$$H_{\text{eq}}(\omega) = \sum_{K=-\infty}^{\infty} H(\tau + kT)\exp(-j\omega kT), \tag{89a}$$

where

$$H(\tau + kT) = \frac{T}{2\pi} \int_{-\pi/T}^{\pi/T} H_{eq}(\omega) \exp(j\omega kT) d\omega. \tag{89b}$$

Assuming the impulse response $H(t)$ has the Fourier transform $H(\omega)$, Poisson's sum formula can be used to get the following relation between the spectra of the sampled and the continuous functions

$$H_{eq}(\omega) = \frac{\exp(j\omega\tau)}{T} \sum_{k=-\infty}^{\infty} H\left(\omega + 2\pi \frac{k}{T}\right) \exp\left(j2\pi k \frac{\tau}{T}\right). \tag{90}$$

Using the spectral density of the filtered noise in baseband

$$|N_{eq}(\omega)|^2 = \sum_{k=-\infty}^{\infty} R_{NN}(kT) \exp[-j(\omega + \omega_0)(kT)] \tag{91}$$

and eqs. (89a) and (89b), the transforms of $\tilde{\mathbf{A}}_1$, $\tilde{\mathbf{A}}_2$, and $\tilde{V}$ can be shown to be

$$\tilde{\mathbf{A}}_1(\omega) = (P_a + P_b)|H_{eq}(-\omega)|^2 + |N_{eq}(-\omega)|^2, \tag{92a}$$

$$\tilde{\mathbf{A}}_2(\omega) = (P_a - P_b) H_{eq}(\omega) H_{eq}(-\omega), \tag{92b}$$

$$\tilde{V}(\omega) = P_a H_{eq}(-\omega). \tag{92c}$$

From eq. (24) and with eqs. (67), (76), and (78) the minimum mse can be expressed as

$$\epsilon_{opt}^2 = P_a - \mathbf{C}_{opt}^t \mathbf{V} = P_a - R_e(\underline{C}^* \underline{V}). \tag{93}$$

In eq. 93, $\underline{C}^* \underline{V}$ can be viewed as the zeroth term of the convolution of the sequences $(\underline{V}_n)$ represented by $\underline{V}$ and (C_{-n}^*) represented by $\underline{C}^*$. Multiplying the spectra and transforming back to time domain yields

$$\mathrm{Re}(\underline{C}^* \underline{V}) = \frac{T}{2\pi} \int_{-\pi/T}^{\pi/T} \frac{1}{2} [C^*(\omega) V(\omega) + C(-\omega) V^*(-\omega)] d\omega. \tag{94}$$

Taking into account the modulation in eqs. (82) and (83), this also can be expressed in terms of $\tilde{C}(\omega)$ and $\tilde{V}(\omega)$, which are defined above.

$$\mathrm{Re}(\underline{C}^* \underline{V}) = \frac{T}{2\pi} \int_{-\pi/T}^{\pi/T} \frac{1}{2} [\tilde{C}(\omega) \tilde{V}(\omega) + \tilde{C}(-\omega) \tilde{V}(-\omega)] d\omega. \tag{95}$$

Combining eqs. (89a), (89b), (92a), (92b), (93), and (95) finally yields the desired expression of the minimum mse

$$\epsilon_{opt}^2 = \frac{TP_a}{2} \int_{-\pi/T}^{\pi/T} \frac{P_b[Z(\omega) + Z(-\omega)] + 1}{\begin{array}{l} 4P_a P_b Z(\omega) \times Z(\omega) \\ \quad + (P_a + P_b) \times [Z(\omega) + Z(\omega)] + 1 \end{array}} d\omega, \tag{96}$$

where

$$Z(\omega) = \left| \frac{H_{eq}(\omega)}{N_{eq}(\omega)} \right|^2. \tag{97}$$

In the balanced power case $P_a = P_b$, we can simplify further to yield

$$\epsilon^2_{opt} = \frac{TP_a}{2\pi} \int_{-\pi/T}^{\pi/T} \frac{1}{2[2P_aZ(\omega) + 1]} + \frac{1}{2[2P_aZ(-\omega) + 1]} d\omega. \tag{98}$$

Since both terms are integrated over one full period this yields

$$\epsilon^2_{opt} = \frac{TP_a}{2\pi} \int_{-\pi/T}^{\pi/T} \frac{d\omega}{2P_aZ(\omega) + 1}. \tag{99}$$

It can be shown that the derivative of the minimum mse eq. (96) with respect to the power in the second branch is

$$\frac{\partial \epsilon^2_{opt}}{\partial P_b} = \frac{TP_a^2}{2\pi} \int_{-\pi/T}^{\pi/T} \frac{[Z(\omega) - Z(-\omega)]^2 d\omega}{D^2}, \tag{100}$$

where D is the denominator of the integrand in eq. (96). This means the derivative is positive unless $Z(\omega)$ is symmetric in which case the former is zero. In general, a decrease in the power of the second branch will decrease the minimum mse in the first branch.

REFERENCES

1. F. Akashi, Y. Sato, and M. Eguchi, unpublished work.
2. T. L. Lim, unpublished work.
3. D. D. Falconer, "Jointly Adaptive Equalization and Carrier Recovery in 2-Dimensional Digital Communication Systems," B.S.T.J., *55* (March 1976), pp. 317–34.
4. D. D. Falconer, "Analysis of a Gradient Algorithm for Simultaneous Passband Equalization and Carrier Phase Recovery," B.S.T.J., *55* (April 1976), pp. 409–28.
5. M. S. Mueller, "Complex Valued Analysis of Cross Coupled Equalizers in Synchronous Data Receivers," (in German) Swiss Federal Inst. of Technology, Ph.D. Thesis 5711, 1976.
6. G. Sandegren, "QAM and SSB Modulation for Data Transmission over Telephone Lines Including Equalizer," Ericsson Technics, *33* (1977), pp. 247–98.
7. H. B. Voelcker, "Toward a Unified Theory of Modulation-Part I: Phase Envelope Relationships," Proc. IEEE, *54* (March, 1966), pp. 340–53.
8. G. Ungerboeck, "Theory on the Speed on Convergence in Adaptive Equalizers for Digital Communications," IBM J. Res. and Dev. (November, 1972), pp. 546–55.